Hierarchical Fast-Slow Singularly Perturbed Nonlinear Control: Application to Soft Multisection Robots.

Lekan Molu

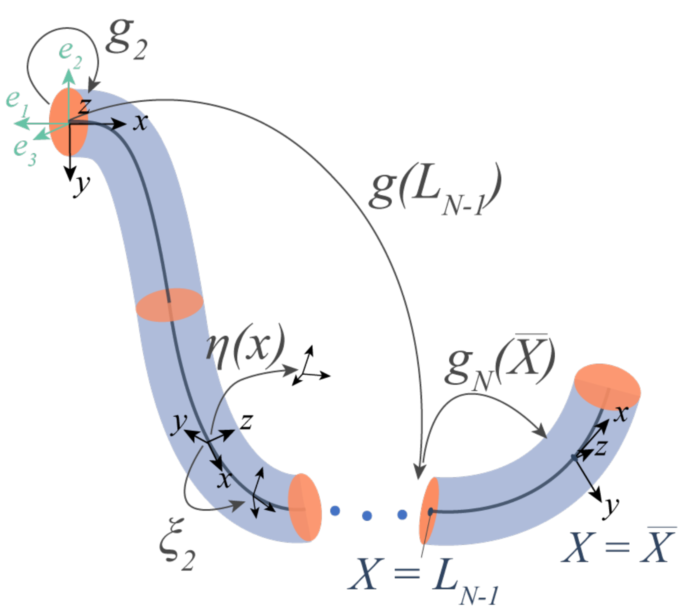

Fig. 1. Configuration schematic of an Octopus robot arm.

***Abstract*— A hierarchical backstepping controller for a nonlinear Newton-Euler soft multisection robot system based on the theory of singularly perturbed systems is here put forward. Decomposing the global system dynamics to a two-time-scale separate subdynamics, we prescribe separate stabilizing controllers for regulating each subsystem's dynamics.**

Supplementary material—All codes for reproducing the experiments reported in this paper are available online: https://github.com/robotsorcerer/dcm.

I. Introduction

II. Notations and Preliminaries

Time variables e.g. t, T, will always be real numbers. Matrices and vectors are respectively upper- and lower-case Roman letters. The strain field and strain twist vectors are Greek letters, that is $\eta \in \mathbb{R}^6$ and $\xi \in \mathbb{R}^3$, respectively. Sets, screw stiffness, wrench tensors, and the gravitational vector are upper-case Calligraphic characters. Distributed wrench tensors are signified with an overbar, e.g. $\bar{\mathcal{F}}$. At time t and for a curve which is the material abscissa $X : [0, L]$[1], the robot's configuration is $\mathcal{X}_t(X)$. The matrix A's Frobenius norm is denoted $\|A\|$ while its Euclidean norm is $\|A\|_2$. The Lie algebra of the Lie group $\mathbb{SE}(3)$ is $\mathfrak{se}(3)$. The special orthogonal group consisting of corkscrew rotations is $SO(3)$. For a configuration $\boldsymbol{g}(X) \in \mathbb{SE}(3)$, its adjoint and coadjoint are respectively $\text{Ad}_{\boldsymbol{g}}$, $\text{Ad}^{\star}_{\boldsymbol{g}}$; these are parameterized by the curve, X. In generalized coordinate, the joint vector of a soft robot is denoted $q = [\xi_1^\top, \ldots, \xi_{n_\xi}^\top]^\top \in \mathbb{R}^{6n_\xi}$.

A. SoRo Configuration

Depicted in Fig. 1, the inertial frame is the basis triad $(\boldsymbol{e}_1, \boldsymbol{e}_2, \boldsymbol{e}_3)$ and $\boldsymbol{g}_r$ is the inertial to base frame transformation. For a cable-driven arm, the point at which actuation occurs is labeled $\bar{X}$. The configuration matrix that parameterizes curve L_n in X is denoted $\boldsymbol{g}_{L_n}$. The cable runs through the z-axis (x-axis in the spatial frame) in the (micro) body frame.

B. Continuous Strain Vector and Twist Velocity Fields

Suppose that $p(X) \in \mathbb{R}^6$ describes a microsolid's position on the soft body at t and let $R(X)$ be the corresponding orientation matrix. Let the pose be $[p(X), R(X)]$. Then, the robot's C-space, parameterized by a curve $g(\cdot) : X \to \mathbb{SE}(3)$, is $g(X) = \begin{pmatrix} R(X) & p(X) \\ \mathbf{0}^\top & 1 \end{pmatrix}$. Suppose that $\varepsilon(X) \in \mathbb{R}^3$ and $\gamma(X) \in \mathbb{R}^3$ respectively denote the linear and angular strain components of the soft arm. Then, the arm's strain field is a state vector, $\breve{\xi}(X) \in \mathfrak{se}(3)$, along the curve $\boldsymbol{g}(X)$ i.e. $\breve{\xi}(X) = \boldsymbol{g}^{-1}\partial g / \partial X \triangleq \boldsymbol{g}^{-1}\partial_x \boldsymbol{g}$. In the microsolid frame, the matrix and vector representation of the strain state are respectively $\breve{\xi}(X) = \begin{pmatrix} \hat{\gamma} & \varepsilon \\ \mathbf{0} & 0 \end{pmatrix} \in \mathfrak{se}(3)$, $\xi(X) = \begin{pmatrix} \gamma^\top & \varepsilon^\top \end{pmatrix}^\top \in \mathbb{R}^6$. Read $\hat{\gamma}$: the anti-symmetric matrix representation of γ. Read $\breve{\xi}$: the isomorphism mapping the twist vector, $\xi \in \mathbb{R}^6$, to its matrix representation in $\mathfrak{se}(3)$. Furthermore, let $\nu(X), \omega(X)$ respectively denote the linear and angular velocities of the curve $g(X)$. Then, the velocity of $\boldsymbol{g}(X)$ is the twist vector field $\breve{\eta}(X) = \boldsymbol{g}^{-1}\partial \boldsymbol{g} / \partial t \triangleq \boldsymbol{g}^{-1}\partial_t \boldsymbol{g}$. In the microsolid frame, $\breve{\eta}(X) = \begin{pmatrix} \hat{\omega} & \nu \\ \mathbf{0} & 0 \end{pmatrix} \in \mathfrak{se}(3)$, $\eta(X) = \begin{pmatrix} \omega^\top & \nu^\top \end{pmatrix}^\top \in \mathbb{R}^6$.

C. Discrete Cosserat-Constitutive PDEs

The PCS model assumes that (ξ_i, η_i) $i = 1, \ldots, N$ robot sections are constant. Spatially spliced along sectional boundaries, the overall strain position and velocity of the entire soft robot is a piecewise sum of the sectional strain field parameters.

The author is with Microsoft Research NYC lekanmolu@microsoft.com.

[1] L is length of the curve.

Using d'Alembert's principle, the generalized dynamics equation for PCS model of Fig. 1 under external and actuation loads admits the form [5]

$$\underbrace{\left[\int_0^{L_N} J^\top \mathcal{M}_a J dX\right]}_{M(q)} \ddot{q} + \underbrace{\left[\int_0^{L_N} J^\top \mathrm{ad}^\star_{J\dot{q}} \mathcal{M}_a J dX\right]}_{C_1(q,\dot{q})} \dot{q} +$$
$$\underbrace{\left[\int_0^{L_N} J^\top \mathcal{M}_a \dot{J} dX\right]}_{C_2(q,\dot{q})} \dot{q} + \underbrace{\left[\int_0^{L_N} J^\top \mathcal{D} J \|J\dot{q}\|_p dX\right]}_{D(q,\dot{q})} \dot{q}$$
$$\underbrace{-\,(1-\rho_f/\rho)\left[\int_0^{L_N} J^\top \mathcal{M} \mathrm{Ad}^{-1}_{\boldsymbol{g}} dX\right]}_{N(q)} \mathrm{Ad}^{-1}_{\boldsymbol{g}_r} \mathcal{G} - \underbrace{J^\top(\bar{X})\mathcal{F}_p}_{F(q)}$$
$$\underbrace{-\int_0^{L_N} J^\top \left[\nabla_x \mathcal{F}_i - \nabla_x \mathcal{F}_a + \mathrm{ad}^\star_{\eta_n}\left(\mathcal{F}_i - \mathcal{F}_a\right)\right] dX}_{\tau(q)} = 0 \tag{1}$$

for a Jacobian $J(X)$, (see definition in [5]), wrench of internal forces $\mathcal{F}_i(X)$, distributed wrench of actuation loads $\bar{\mathcal{F}}_a(X)$, and *distributed* wrench of the applied external forces $\bar{\mathcal{F}}_e(X)$. The torque and (internal) force are respectively M_k, F_k for sections k; and $\mathcal{M}(X)$ is the screw mass inertia matrix, given as $\mathcal{M}(X) = \mathrm{diag}\left(I_x, I_y, I_z, A, A, A\right)\rho$ for a body density ρ, sectional area A, bending, torsion, and second inertia operator I_x, I_y, I_z respectively.

Equation (1) can be appropriately written in standard Newton-Euler (N-E) form as

$$\begin{aligned} M(q)\ddot{q} + \left[C_1(q,\dot{q}) + C_2(q,\dot{q})\right]\dot{q} = \tau(q) + F(q) \\ + N(q)\mathrm{Ad}^{-1}_{\boldsymbol{g}_r}\mathcal{G} - D(q,\dot{q})\dot{q}. \end{aligned} \tag{2}$$

In (1), $\mathcal{M}_a = \mathcal{M} + \mathcal{M}_f$ is a lumped sum of the microsolid mass inertia operator, $\mathcal{M}$, and that of the added mass fluid, $\mathcal{M}_f$; dX is the length of each section of the multi-robot arm; $\mathcal{D}(X)$ is the drag fluid mass matrix; $J(X)$ is the Jacobian operator; $\|\cdot\|_p$ is the translation norm of the expression contained therein; ρ_f is the density of the fluid in which the material moves; ρ is the body density; $\mathcal{G}$ is the gravitational vector defined as $\mathcal{G} = \left[0, 0, 0, -9.81, 0, 0\right]^T$; and $\mathcal{F}_p$ is the applied wrench at the point of actuation $\bar{X}$. These terms form the overall mass $M(q)$, Coriolis forces $C_i(q,\dot{q}), i = 1, 2$, buoyancy-gravitational forces $N(q)$, drag matrix $D(q,\dot{q})$ and external force $F(q)$ in (2).

Suppose that

$$z = \begin{pmatrix} z_1 & z_2 \end{pmatrix}^\top \equiv \begin{pmatrix} q & \dot{q} \end{pmatrix}^\top \tag{3}$$

then we may transform (2) into the following set of first-order differential equations

$$\dot{z}_1 = z_2, \tag{4a}$$
$$\dot{z}_2 = M^{-1}\left\{\tau - (C_1 + C_2 + D)z_2 + F + N\mathrm{Ad}^{-1}_{\boldsymbol{g}_r}\mathcal{G}\right\}, \tag{4b}$$

where we have omitted the templated arguments for simplicity. We refer readers to Renda et al. [5], Boyer and Renda [1], Renda et al. [4] for further details.

III. Hierarchical Control Scheme

Our goal is to design a *multi-resolution feedback control scheme* which steer an arbitrary point in the joint space, $q(t)$ at time t, to a target point $q^d = (q_1^d, \ldots, q_N^d)^\top$[2] based on backstepping control design. Owing to the long computational times required to realize effective control [2], we transform the Cosserat system into a singularly perturbed system. Under standard singular perturbation theory (SPT) assumptions, we take a composite control system viewpoint – separating fast and slow dynamics as we decompose (2) into a nonlinear two time-scale system comprising separate fast and slow controllers.

A. Singularly Perturbed Composite Controller

Seeking a robust response to parametric variations, noise sensitivity, and parasitic "small" time constants components of the dynamics that increase model order, we separate the fast- (i.e. z_2) from the slow-changing (i.e. z_1) dynamics of (2). Thus, we write

$$\dot{z}_1 = f(z_1, z_2, \epsilon, u_s, t),\ z_1(t_0) = z_1(0),\ z_1 \in \mathbb{R}^{6N} \tag{5a}$$
$$\epsilon\dot{z}_2 = h(z_1, z_2, \epsilon, u_f, t),\ z_2(t_0) = z_2(0),\ z_2 \in \mathbb{R}^{6N} \tag{5b}$$

where f and h are $\mathcal{C}^n (n \gg 0)$ differentiable functions of their arguments, $\epsilon > 0$ denotes all small parameters to be ignored[3], u_s is the slow sub-dynamics' control law, and u_f is the fast sub-dynamics' controller.

Let us set $\epsilon = 0$; this reduces the system's dimension so that (5b) becomes the algebraic equation

$$0 = h(\bar{z}_1, \bar{z}_2, 0, u_s, t) \tag{6}$$

where $\bar{(\cdot)}$ signifies a variable in the system with $\epsilon = 0$. We proceed with the following assumptions.

Assumption 1 (Real and distinct root): Equation (6) has a unique and distinct root, given as $\bar{z}_2 = \phi(\bar{z}_1, t)$. Substituting $\bar{z}_2$ into (6), we have the form

$$0 = h(\bar{z}_1, \phi(\bar{z}_1, t), 0, u_s, t) \triangleq \bar{h}(\bar{z}_1, u_s, t),\ \bar{z}_1(t_0) = z_1(0), \tag{7}$$

where we have chosen the initial condition of the original system. Thus, the *quasi steady-state* (or slow) subsystem is

$$\dot{\bar{z}}_1 = f(\bar{z}_1, \bar{h}(\bar{z}_1, u_s, t), 0, u_s, t) \triangleq f_s(\bar{z}_1, u_s, t). \tag{8}$$

The variation of the slow subsystem (8) from the original system's response constitutes the fast transient $\tilde{z}_2 = z_2 - \bar{h}(\bar{z}_1, u_s, t)$ on a time scale $T = t/\epsilon$ so that

$$\frac{dz_1}{dT} = \epsilon f(z_1, z_2, \epsilon, u_s, t), \tag{9a}$$
$$\begin{aligned} \frac{d\tilde{z}_2}{dT} &= \epsilon\frac{dz_2}{dt} - \epsilon\frac{\partial\bar{h}_1}{\partial\bar{z}_1}\dot{\bar{z}}_1, \\ &= h(z_1, \tilde{z}_2 + \bar{h}(\bar{z}_1, u_s, t), \epsilon, u_f, t) - \epsilon\frac{\partial\bar{h}_1}{\partial\bar{z}_1}\dot{\bar{z}}_1. \end{aligned} \tag{9b}$$

When $\epsilon = 0$, for the fast subsystem we must have

$$\frac{d\tilde{z}_2}{dT} = h(z_1, \tilde{z}_2 + \bar{h}(\bar{z}_1, u_s, t), 0, u_f, t). \tag{10}$$

[2]Here, q_i is the joint space for a section of the multisection manipulator.

[3]Restriction to a two-time-scale is not binding and one can choose to expand the system into multiple sub-dynamics across multiple time scales.

B. Singularly Perturbed SoRo Dynamics

First, consider a cable-actuated robot. At the point $\bar{X}$ (see Fig. 1) for the configuration $\mathcal{X}_t(\bar{X})$, the robot's motion is principally a consequence of the deformation of microslids around $\mathcal{X}_t(\bar{X})$. Denote the composite mass of these microsolids as $\mathcal{M}^{\text{core}}$. The motion of every other microsolid (with mass $\mathcal{M}^{\text{pert}}$) can be considered a perturbation from $\mathcal{M}^{\text{core}}$ so that $\mathcal{M}^{\text{pert}} = \mathcal{M} \setminus \mathcal{M}^{\text{core}}$. For fluid-driven robots' deformation such as fiber reinforced elastomeric enclosures (FREEs) with deformable shells [6, 3], principal motion is a consequence of deformation near the actuation area; let the core mass of these microsolids be $\mathcal{M}^{\text{core}}$). And let $\mathcal{M}^{\text{pert}}$ constitute the mass of the remnant micro-solids.

On a first glance at (1), it may seem that separating the slow and fast portions of the matrices $M(q)$, $C_1(q,\dot{q})$, $C_2(q,\dot{q})$ and $N(q)$ with different perturbation parameters is the most straightforward separation scheme. However, on a closer observation, the integro-matrices have in common the distributed mass density $\mathcal{M}$. Thus, we can choose a uniform perturbation parameter, $\epsilon = \|\mathcal{M}^{\text{core}}\|/\|\mathcal{M}^{\text{pert}}\|$ for separating the system dynamics.

The matrix densities of interest are separable as follows

$$M(q) = M^c(q) + M^p(q), \tag{11a}$$
$$C_1(q,\dot{q}) = C_1^c(q,\dot{q}) + C_1^p(q,\dot{q}), \tag{11b}$$
$$C_2(q,\dot{q}) = C_2^c(q,\dot{q}) + C_2^p(q,\dot{q}), \tag{11c}$$
$$N(q) = N^c(q) + N^p(q), \tag{11d}$$

where $(\cdot)^c, (\cdot)^p$ respectively denote the core and perturbed matrices over abscissa indices $[L^c_{\text{min}}, L^c_{\text{max}}]$ and $[L^p_{\text{min}}, L^p_{\text{max}}]$, respectively. Given the robot configuration in Fig. 1, we choose $0 \le L^p_{\text{min}} < L^c_{\text{min}}$ and $L^c_{\text{max}} < L^p_{\text{max}} \le L$. We write the singularly perturbed form of (4) as

$$\dot{z}_1 = z_2, \tag{12a}$$
$$\begin{aligned}\epsilon M\dot{z}_2 = \tau(z_1) + F(z_1) + N(z_1)\text{Ad}^{-1}_{\boldsymbol{g}_r}\mathcal{G} - \\ \left[C_1(z_1,z_2) + C_2(z_1,z_2) + D(z_1,z_2)\right] z_2. \end{aligned}\tag{12b}$$

The justification for this model is described in what follows.

1) Quasi steady-state sub-dynamics extraction: Following the arguments in the foregoing, on the perturbed microsolids deformation is minute so that the strain twists and acceleration dynamics i.e. $(\dot{z}_1, \dot{z}_2)$ are equally small. Thus, for the slow subdynamics (4) transforms into

$$\dot{z}_1 = z_2, \tag{13a}$$
$$\begin{aligned}\epsilon M^p(z_1)\dot{z}_2 = \tau(z_1) + F(z_1) + N^p(z_1)\text{Ad}^{-1}_{\boldsymbol{g}_r}\mathcal{G} - \\ \left[C^p_1(z_1,z_2) + C^p_2(z_1,z_2) + D(z_1,z_2)\right] z_2.\end{aligned}\tag{13b}$$

For $\epsilon = 0$, the resulting algebraic equation is

$$\begin{aligned}\tau(\bar{z}_1) + F(\bar{z}_1) + N^p(\bar{z}_1)\text{Ad}^{-1}_{\boldsymbol{g}_r}\mathcal{G} - \\ \left[C^p_1(\bar{z}_1,\bar{z}_2) + C^p_2(\bar{z}_1,\bar{z}_2) + D(\bar{z}_1,\bar{z}_2)\right] \bar{z}_2 = 0\end{aligned} \tag{14}$$

so that

$$\begin{aligned}\bar{z}_2 = \left[C^p_1(\bar{z}_1,\bar{z}_2) + C^p_2(\bar{z}_1,\bar{z}_2) + D(\bar{z}_1,\bar{z}_2)\right]^{-1} \{\tau(\bar{z}_1) \\ + F(\bar{z}_1) + N(\bar{z}_1)\text{Ad}^{-1}_{\boldsymbol{g}_r}\mathcal{G}\}\end{aligned} \tag{15}$$

where the bar signifies variables within the reduced system. Thus, the slow subsystem can be written as

$$\begin{aligned}\dot{\bar{z}}_1 &= \bar{z}_2, \\ &\triangleq \left[C^p_1(\bar{z}_1,\bar{z}_2) + C^p_2(\bar{z}_1,\bar{z}_2) + D(\bar{z}_1,\bar{z}_2)\right]^{-1} \{\tau(\bar{z}_1) \\ &\quad + F(\bar{z}_1) + N(\bar{z}_1)\text{Ad}^{-1}_{\boldsymbol{g}_r}\mathcal{G}\}.\end{aligned} \tag{16}$$

2) Fast subsystem dynamics extraction: The residual of the original system from the slow subsystem i.e. $\tilde{z}_2 = z_2 - \bar{z}_2$ is the fast transient on a time scale $T = t/\epsilon$. The fastest subsystem's dynamics evolves as

$$\frac{dz_1}{dT} = \epsilon z_2, \quad T = t/\epsilon, \tag{17a}$$
$$\begin{aligned}(M^c(z_1) + \epsilon\Lambda^m)\frac{d\tilde{z}_2}{dT} = \tau(z_1) + F(z_1) + (N^c(z_1) + \\ \epsilon\Lambda^n)\text{Ad}^{-1}_{\boldsymbol{g}_r}\mathcal{G} - (C^c_1 + \epsilon\Lambda^c_1 + C^c_2 + \epsilon\Lambda^c_2 + D)\, z_2\end{aligned} \tag{17b}$$

where we have occasionally omitted the templated arguments for ease of notation, and $\Lambda^m = M^p/\epsilon$, $\Lambda^c_1 = C^p_1/\epsilon$, $\Lambda^c_2 = C^p_2/\epsilon$, $\Lambda^n = N^p/\epsilon$, for $\epsilon = \|\mathcal{M}^{\text{core}}\|/\|\mathcal{M}^{\text{pert}}\|$ and the matrix $(M^c + \epsilon\Lambda^m)$ is assumed to be invertible. Carrying out the standard $\epsilon = 0$ on the fast time scale, we find that

$$\frac{dz_1}{dT} = 0, \tag{18a}$$
$$\begin{aligned}M^c(z_1)\frac{d\tilde{z}_2}{dT} = \tau(z_1) + F(z_1) + N^c(z_1)\text{Ad}^{-1}_{\boldsymbol{g}_r}\mathcal{G} - \\ \left[C^c_1(z_1,\tilde{z}_2) + C^c_2(z_1,\tilde{z}_2) + D(z_1,\tilde{z}_2)\right]\tilde{z}_2.\end{aligned} \tag{18b}$$

C. Fast-Slow Backstepping Controller and Stability Analyses

We proceed to design nonlinear backstepping controllers for the two separate time-scale problems developed in §III-B. For the standard Lyapunov comparison function assumptions that guide our design, we refer readers to Appendix I.

1) Slow Subsystem's Stability Analysis: Suppose that we define a virtual input ρ for the slow subsystem (16) so that $\dot{\bar{z}}_1 = \rho$. The tracking errors and corresponding error dynamics are

$$e_1 = z_1 - q^d, \quad \bar{e}_1 = \bar{z}_1 - q^d, \tag{19a}$$
$$\dot{e}_1 = \dot{z}_1 - \dot{q}^d, \quad \dot{\bar{e}}_1 = \dot{\bar{z}}_1 - \dot{q}^d; \tag{19b}$$

where we have used the same desired joint trajectory, q^d, for the full first subsystem and its variant when $\epsilon = 0$. Consider the Lyapunov function candidate,

$$V(z_1) = \frac{1}{2}e_1^\top K_p e_1 \tag{20}$$

where K_p is a matrix of positive damping (gains). Thus,

$$\dot{V}(z_1) = \frac{\partial V}{\partial e_1}\dot{\bar{e}}_1 + \frac{\partial V}{\partial e_1}(\dot{e}_1 - \dot{\bar{e}}_1), \tag{21a}$$
$$= e_1^\top K_p \dot{\bar{e}}_1 + e_1^\top K_p(\dot{e}_1 - \dot{\bar{e}}_1), \tag{21b}$$
$$= e_1^\top K_p(\rho - \dot{q}^d) + e_1^\top K_p(\dot{z}_1 - \dot{\bar{z}}_1). \tag{21c}$$

Suppose that we set $\rho = \dot{q}^d - e_1$, we must have

$$\dot{V}(z_1) \le -e_1^\top K_p e_1 + e_1^\top K_p(z_2 - \bar{z}_2), \tag{22a}$$
$$\le -e_1 K_p(e_1 - \tilde{z}_2), \tag{22b}$$

where $\tilde{z}_2$ prescribes the growth of $\dot{z}_1$ in $\bar{z}_2$. Thus, we have for all $t \geq 0$, that $z_1(t) \in S$ for a compact subset S of $\mathbb{R}^{6N}$. Hence, $z_1(t)$ remains bounded as $t \to \infty$. and we conclude that the origin is asymptotically stable under the virtual input $\rho = \dot{q}^d - e_1$.

2) Boundary layer subsystem's stability analysis: For the boundary layer system (18), define $e_2 = \tilde{z}_2 - \rho$ so that

$$\dot{e}_2 = \dot{\tilde{z}}_2 - \dot{\rho} = \dot{\tilde{z}}_2 - \ddot{q}^d + \dot{e}_1. \tag{23}$$

From (19), we have $\dot{e}_1 = z_2 - \rho + \rho - \dot{q}^d \triangleq e_2 - e_1$. Hence,

$$\dot{e}_2 = \dot{\tilde{z}}_2 - \ddot{q}^d + e_2 - e_1. \tag{24}$$

On the time-scale $T = t/\epsilon$, choose the following Lyapunov function candidate

$$W(z_1, z_2) = \frac{1}{2}\{e_2^\top M e_2 + e_1^\top K_p e_1\}, \tag{25}$$

where $W(z_1, z_2) > 0 \,\forall (z_2 \neq \bar{z}_2)$, z_1 is fixed, and $W(z_1, \bar{z}_2) = 0$. It follows that

$$\frac{dW}{dT}(z_1, z_2) = \frac{1}{\epsilon}\left\{\frac{\partial W}{\partial e_1}\dot{e}_1 + \frac{\partial W}{\partial e_2}\dot{e}_2\right\}, \tag{26a}$$

$$= \frac{1}{\epsilon}e_1^\top K_p(e_2 - e_1) + \frac{1}{\epsilon}e_2^\top M\frac{de_2}{dT} + \frac{1}{2\epsilon}e_2^\top\frac{dM}{dT}e_2. \tag{26b}$$

Let us parameterize the full controller as

$$\begin{aligned}\tau(z_1) = M^c\frac{d\rho}{dT} + [C_1^c(z_1, \tilde{z}_2) + C_2^c(z_1, \tilde{z}_2)]\rho + D(z_1, \tilde{z}_2)\tilde{z}_2 \\ - (F(z_1) + N^c(z_1)\mathrm{Ad}_{\boldsymbol{g}_r}^{-1}\mathcal{G}) + u(z_1, \tilde{z}_2)\end{aligned} \tag{27}$$

where $u(z_1, \tilde{z}_2)$ is the residual control to be designed. Setting $\breve{C}^c(z_1, \tilde{z}_2) = C_1^c(z_1, \tilde{z}_2) + C_2^c(z_1, \tilde{z}_2)$, and plugging (27) into (4), we have

$$M^c\frac{d}{dT}(\tilde{z}_2 - \rho) + \breve{C}^c(z_1, \tilde{z}_2)(\tilde{z}_2 - \rho) = u(z_1, \tilde{z}_2) \tag{28}$$

so that (26) becomes

$$\begin{aligned}\frac{dW}{dT} &= \frac{1}{\epsilon}\left\{e_1^\top K_p(e_2 - e_1) + e_2^\top M\left(u(z_1, \tilde{z}_2) - \breve{C}e_2\right)\right\} \\ &\quad + \frac{1}{2\epsilon}e_2^\top\frac{dM}{dT}e_2 \\ &= \frac{1}{\epsilon}\left\{-e_1^\top K_p e_1 + e_2^\top\left(K_p e_1 + u(z_1, \tilde{z}_2)\right)\right\}\end{aligned} \tag{29}$$

where we have employed the skew-symmetric property, $dM/dT - 2\breve{C}(z_1, \tilde{z}_2) = 0$ (an extension to the time scale $T = t/\epsilon$ of the proof in [2]) to arrive at the above. If we set $u(z_1, \tilde{z}_2) = -K_p e_1 - M e_2$, then we must have

$$\frac{dW}{dt} = -e_1^\top K_p e_1 - e_2^\top M e_2 \triangleq -2W(z_1, z_2). \tag{30}$$

Hence, exponential stability follows as a result of the controller

$$\begin{aligned}\tau &= M^c(z_1)(\dot{\rho} - e_2) + \breve{C}^c(z_1, \tilde{z}_2)\rho \\ &\quad + D(z_1, \tilde{z}_2)\tilde{z}_2 - (F + N^c(z_1)\mathrm{Ad}_{\boldsymbol{g}_r}^{-1}\mathcal{G}) - K_p e_1\end{aligned} \tag{31}$$

since $M(z_1)$ is positive definite and bounded from below as shown in [2], $M^c(z_1)$ is also positive. Since $\dot{\rho} = \ddot{q}_d - \dot{e}_1 = \ddot{q}_d - (e_2 - e_1)$, the controller in (31) also admits the form

$$\begin{aligned}\tau &= M^c(q)(\ddot{q}_d - 2e_2 + e_1) + \breve{C}^c(q, \dot{q})(q_d - e_1) \\ &\quad + D(q)\dot{q} - F(q) - N^c(q)\mathrm{Ad}_{\boldsymbol{g}_r}^{-1}\mathcal{G} - K_p e_1,\end{aligned} \tag{32}$$

IV. Numerical Results

V. Discussions and Conclusion

References

[1] Frederic Boyer and Federico Renda. Poincaré's equations for cosserat media: application to shells. *Journal of Nonlinear Science*, 2016. 2

[2] Lekan Molu, Shaoru Chen, and Audrey Sedal. Lagrangian Properties and Control of Soft Robots Modeled with Discrete Cosserat Rods. *(submitted to) IEEE International Conference on Robotics and Automation*, 2023. URL https://scriptedonachip.com/downloads/Papers/SoRoPD.pdf. 2, 4

[3] Olalekan Ogunmolu, Xinmin Liu, Nicholas Gans, and Rodney D Wiersma. Mechanism and model of a soft robot for head stabilization in cancer radiation therapy. In *2020 IEEE International Conference on Robotics and Automation (ICRA)*, pages 4609–4615. IEEE, 2020. 3

[4] Federico Renda, Vito Cacucciolo, Jorge Dias, and Lakmal Seneviratne. Discrete cosserat approach for soft robot dynamics: A new piece-wise constant strain model with torsion and shears. *IEEE International Conference on Intelligent Robots and Systems*, 2016-Novem:5495–5502, 2016. ISSN 21530866. 2

[5] Federico Renda, Frédéric Boyer, Jorge Dias, and Lakmal Seneviratne. Discrete cosserat approach for multisection soft manipulator dynamics. *IEEE Transactions on Robotics*, 34(6):1518–1533, 2018. 2

[6] Audrey Sedal, Daniel Bruder, Joshua Bishop-Moser, Ram Vasudevan, and Sridhar Kota. A continuum model for fiber-reinforced soft robot actuators. *Journal of Mechanisms and Robotics*, 10(2):024501, 2018. 3

Appendix I
Lyapunov Stability Assumptions

*Assumption 2 (**Solution assumptions**):* We make the following assumptions about Lyapunov function candidates for the reduced (16), boundary layer (18), and the full singularly perturbed system (12).

- For all $t \geq 0$, $z_1(t) \in S$ where S is a compact subset of $\mathbb{R}^{6N}$. This assures that $z_1(t)$ remains bounded as $t \to \infty$;
- The origin of (12) is an isolated equilibrium in $\mathbb{R}^{6N} \times \mathbb{R}^{6N}$ i.e.

$$0 = z_2, \tag{I.1a}$$

$$0 = \tau(0) + F(0) + N(0)\mathrm{Ad}_{\boldsymbol{g}_r}^{-1}\mathcal{G}; \tag{I.1b}$$

and

- $z_2 = h(z_1)$ is a unique root of (I.1b) where $h(z_1)$ is a sufficiently many times continuously differentiable function of z_1.

Let us now consider comparison inequalities imposed on the Lyapunov functions of the slow and fast subdynamics respectively.

Assumption 3 (Boundary Layer's Lyapunov Candidate): The boundary layer system (18) admits a Lyapunov function candidate $W(z_1, z_2)$ (whereupon z_1 is treated as a fixed parameter) such that for all $(z_1, z_2) \in \mathbb{R}^{6N} \times \mathbb{R}^{6N}$, the following holds

(i) $W(z_1, z_2) > 0 \ \forall \ z_2 \neq \bar{z}_2$ and $W(z_1, \bar{z}_2) = 0$,

(ii) $\dfrac{\partial W}{\partial z_1}\dot{z}_1 \leq \gamma\phi^2(z_2 - \bar{z}_2) + \beta_2\psi(z_1)\phi(z_2 - \bar{z}_2)$,

(iii) $\dfrac{\partial W}{\partial z_2}\dot{z}_2 \leq -\dfrac{1}{\epsilon}\alpha_2 M^{-1}\phi^2(z_2 - \bar{z}_2), \quad \alpha_2 > 0$,

where $\psi(z_1)$ and $\phi(\cdot)$ are scalar functions which vanish when their vector arguments are zero; and γ and β_2 can be positive, zero, or negative. Note that the condition (ii) above implies that $\bar{z}_2$ is an origin (this also follows from (I.1a)).

Assumption 4 (Slow subsystem's Lyapunov Candidate): Let us rewrite (12a) as

$$\dot{z}_1 = \bar{z}_2 + z_2 - \bar{z}_2 \tag{I.2}$$

where $z_2 - \bar{z}_2$ is the reduced system (8)'s perturbation. Let a Lyapunov function candidate $V(z_1)$ exist so that the following inequality

$$\frac{\partial V}{\partial z_1}\dot{\bar{z}}_1 \leq -\alpha_1\psi^2(z_1) \quad \alpha_1 > 0, \tag{I.3}$$

assures that $\bar{z}_1 = 0$ is an asymptotically stable equilibrium. Then,

$$\begin{aligned}\frac{\partial V}{\partial z_1}\dot{z}_1 &= \frac{\partial V}{\partial z_1}\dot{\bar{z}}_1 + \frac{\partial V}{\partial z_1}(\dot{z}_1 - \dot{\bar{z}}_1) \\ &\leq -\alpha_1\psi^2(z_1) + \frac{\partial V}{\partial z_1}(z_2 - \bar{z}_2).\end{aligned} \tag{I.4}$$

If we prescribe the growth of $\dot{z}_1$ in $\bar{z}_2$ by $\dfrac{\partial V}{\partial z_1}(z_2 - \bar{z}_2) \leq \beta_1\psi(z_1)\phi(z_2 - \bar{z}_2)$, then

$$\dot{V} \leq -\alpha_1\psi^2(z_1) + \beta_1\psi(z_1)\phi(z_2 - \bar{z}_2). \tag{I.5}$$

Assumption 5 (Global Lyapunov Function Candidate): Given assumptions 3 and 4, there exists a convex combination of the separate Lyapunov functions which can be prescribed for the singularly perturbed system (11) as

$$\Lambda(z_1, z_2) = (1 - \sigma)V(z_1) + \sigma W(z_1, z_2), \ 0 < \sigma < 1, \tag{I.6}$$

Along the trajectories of (11), it follows that

$$\frac{d\Lambda}{dt} = (1-\sigma)\frac{\partial V}{\partial z_1}\dot{z}_1 + \frac{\sigma}{\epsilon}\frac{\partial W}{\partial z_1}\dot{z}_1 + \sigma\frac{\partial W}{\partial z_2}\dot{z}_2 \tag{I.7}$$

$$\begin{aligned}&= (1-\sigma)\left[\frac{\partial V}{\partial z_1}\dot{\bar{z}}_1 + \frac{\partial V}{\partial z_1}(\dot{z}_1 - \dot{\bar{z}}_1)\right] + \\ &\quad \frac{\sigma}{\epsilon}\frac{\partial W}{\partial z_1}\dot{z}_1 + \sigma\frac{\partial W}{\partial z_2}\dot{z}_2 \\ &\leq (1-\sigma)\left[\alpha_1\psi^2(z_1) - \beta_1\psi(z_1)\phi(z_2 - \bar{z}_2)\right] + \\ &\quad \frac{\sigma}{\epsilon}\left[\gamma\phi^2(z_2 - \bar{z}_2) + \beta_2\psi(z_1)\phi(z_2 - \bar{z}_2)\right. \\ &\quad \left. -\epsilon\alpha_2 M^{-1}\phi^2(z_2 - \bar{z}_2)\right]\end{aligned} \tag{I.8}$$